Available online at www.sciencedirect.com

SCIENCE DIRECT

Metabolism Clinical and Experimental 54 (2005) 682–688

Metabolism
Clinical and Experimental

www.elsevier.com/locate/metabol

Absence of fatty liver in familial hypobetalipoproteinemia linked to chromosome 3p21

Pin Yue, Tariq Tanoli, Olayinka Wilhelm, Bruce Patterson, Dmitriy Yablonskiy, Gustav Schonfeld*

Departments of Internal Medicine and Radiology, Washington University School of Medicine, St Louis, MO 63110, USA

Received 27 August 2004; accepted 5 December 2004

Abstract

Our aim was to ascertain whether fatty liver may be present in the genetic form of familial hypobetalipoproteinemia (FHBL) linked to a susceptibility locus on chromosome 3p21. Three genetic forms of FHBL exist: (a) FHBL caused by truncation-specifying mutations of apolipoprotein B (apoB), (b) FHBL linked to chr3p21, and (c) FHBL not linked either to *APOB* or to chr3p21. Fatty liver is common in apoB-defective FHBL.

Hepatic fat contents were quantified by magnetic resonance spectroscopy in 16 subjects with 3p21-linked FHBL, 32 subjects with apoB-defective FHBL, and 39 sex- and age-matched controls. Mean liver fat of 3p21 subjects was similar to controls and approximately 60% lower than apoB-defective FHBL subjects ($P = .0012$). Indices of adiposity (body mass index, waist/hip ratio) and masses of abdominal subcutaneous, retroperitoneal, and intraperitoneal adipose tissue (IPAT) were quantified by MR imaging. Mean measures of adiposity were similar in the 3 groups, suggesting that adiposity per se was not responsible for differences in liver fat. Liver fat content was positively correlated with IPAT. The intercepts of regression lines of IPAT on liver fat content were similar in controls and 3p21, but higher in apoB-defective FHBL subjects. The slopes of the lines were steepest in apoB-defective, intermediate in 3p21, and flattest in controls. Lipoprotein profiles and very low density lipoprotein–apoB100 kinetics of 3p21 and apoB-defective groups also differed. Thus, 2 genetic subtypes of FHBL also differ in several phenotypic features.

1. Introduction

Although fatty liver is common in one genetic form of familial hypobetalipoproteinemia (FHBL) [1-4], it is not clear whether this is true for all genetic forms. At least 3 genetic forms of FHBL exist. Of these, the best characterized consists of families harboring a variety of genetic mutations of *APOB* (chromosome 2) [5]. The overwhelming majority of these autosomal dominant mutations specifies the synthesis of truncated forms of apolipoprotein B (apoB) ranging from apoB2 to apoB89, based on a centile nomenclature in which the full-length hepatic protein consisting of 4536 amino acid residues is designated as apoB100 and the naturally truncated intestinal apoB is designated as apoB48 [6]. In addition, amino acid substitutions in critical lipid binding regions of *APOB* may result in FHBL [7]. The second genetic form, also segregating as a dominant, was described in 7 families. In these families, the low low-density lipoprotein (LDL) cholesterol/apoB levels were linked to a susceptibility locus on chromosome 3p21 [8,9], although the gene has not yet been identified. The third form also apparently dominant was found in 9 families in which linkage to chromosomes 2 and 3 were excluded [5].

The apoB-defective subjects, as a group, have liver fat contents that are approximately 3 times higher than those of control subjects with normal plasma lipid levels, matched for age, body mass index (BMI), and sex [2]. Although in both apoB-defective FHBL subjects and in matched controls, liver fat contents increase directly with the sizes of the intraperitoneal fat depots and the area under the curve (AUC) for insulin during oral glucose challenge, the rise in liver fat is greater in subjects with FHBL; that is, for any given magnitude of intraperitoneal fat mass or AUC insulin, apoB-defective FHBL subjects have significantly greater amounts of liver fat than controls [2]. This suggests that these FHBL subjects are genetically more susceptible than

* Corresponding author. Tel.: +1 314 362 7038; fax: +1 314 747 4477.
E-mail address: gschonfe@im.wustl.edu (G. Schonfeld).

0026-0495/$ – see front matter © 2005 Elsevier Inc. All rights reserved.
doi:10.1016/j.metabol.2004.12.013

control subjects to metabolic/lifestyle factors that would tend to raise liver fats.

It is highly likely that the increased susceptibility to fatty liver in subjects with apoB-defective FHBL is caused by lower than normal very low density lipoprotein (VLDL)–apoB100 and VLDL-triglycerides (TG) production rates that limit the capacity of the hepatic export system for TG, resulting in the accumulation of TG in the liver [10]. LDL-apoB100 and VLDL-TG production rates were also low in subjects with 3p21-linked form of FHBL. However, the fractional catabolic rates (FCRs) of both VLDL components were higher in the 3p21 group than either control or apoB-defective groups [11]. To assess whether the different VLDL kinetics in the 3p21-linked form of FHBL also would be accompanied by differences in liver fat content, we examined the hepatic fat contents of 3p21-linked FHBL subjects, using magnetic resonance spectroscopy (MRS). Furthermore, to assess and compare the correlations between hepatic fat contents and the measurements of obesity and insulin action in 3p21-linked and apoB-defective FHBL subjects, we concomitantly measured indices of general and abdominal adiposity (MR imaging [MRI]) and insulin action. Although the indices of insulin action and adiposity were similar in controls, apoB-defective FHBL subjects, and 3p21 subjects, mean liver fat contents of 3p21 subjects were lower than those of apoB-defective subjects and similar to those of controls. Thus, significant phenotypic differences exist in hepatic TG metabolism of these 2 genetic subtypes of FHBL.

2. Materials and methods

2.1. Study subjects, protocols, and routine chemistries

The Washington University Human Studies Committee approved our experimental protocols and consenting procedures. Subjects were not acutely ill, nor were they taking medicines known to affect lipid metabolism. We have previously reported on subjects with the apoB-deficient forms of FHBL and matched controls [1,2]. The descriptions of the "3p21 linkage" families and subjects have been published [8,9]. The study subjects reported here are enumerated in the footnote to Table 1. The controls are matched for age, sex, and indices of obesity. Thirty-three of 39 were included in the previous report [2]. No upper "normal" limit on the liver fat content of our control group was set because the amount of liver fat was continuously distributed. The control group contains subjects who could be designated as having fatty livers based on the frequently used cut point of liver fat, 5% [12].

Plasma lipids and lipoproteins were quantified by enzymatic methods (Wako Chemicals, Richmond, Va) on plasmas obtained after 12-hour fasting, after separation of lipoproteins by combined ultracentrifugal and precipitation methods according to the Lipid Research Clinic protocols [13]. Liver chemistry profiles were normal. ApoB and apoA1 levels were determined by immunonephelometry [14]. Oral glucose tolerance tests were performed 12 hours after fasting with 75 g of glucose. Plasma glucose and insulin were analyzed in the Core Laboratory of the Washington University General Clinical Research Center. For the MRS study, subjects were instructed not to change their diets and to abstain from ethanol for at least 1 week before the studies. MRS and MRI studies were usually performed after fasting 10 to 12 hours. Diurnal variation of liver fat is small [1].

2.2. Abdominal fat masses by MRI

The procedure was described previously [2]. Briefly, a 1.5-T Siemens Magnetom Vision scanner (Siemens, Erlangen, Germany) was used. Axial MRI images of the abdomen were obtained in a body coil. Gradient echo sequences were used with repetition time of 160 milliseconds and echo time of 2.7 milliseconds. Images were acquired on a 116 × 256 matrix within a 33.8 × 45.0 cm^2 field of view. The "Analyze 3.1" image analysis software program (Biomedical Imaging Resource) was used for quantification of adipose tissue volume. Eight contiguous slices (first slice from the top of the right kidney; in deep inspiration, these slices usually correspond to vertebra levels L1, L2, and L3) were used for quantification of subcutaneous adipose tissue (SAT) and intra-abdominal adipose tissue. Intra-abdominal adipose tissue was divided into retroperitoneal adipose tissue (RPAT) and intraperitoneal adipose tissue (IPAT) compartments using anatomic structures, such as pancreas, ascending and descending colon, inferior vena cava, and aorta as markers.

Table 1
Clinical characteristics of study subjects in the 3 groups

Subjects (men/women)	Liver fat (%)	Age (y)	Total TG (mg/dL)	VLDL-TG (mg/dL)	Total cholesterol (mg/dL)	VLDL-C (mg/dL)	LDL-C (mg/dL)	HDL-C (mg/dL)	ApoAI (mg/dL)	ApoB (mg/dL)
Control (17/22)	4.7 ± 5.5[a]	40 ± 15	101 ± 67[a]	72 ± 67[a]	171 ± 31[a]	16 ± 12[a]	108 ± 26[a]	46 ± 11[a]	121 ± 23[a]	82 ± 28[a]
ApoB truncation (18/16)	14.8 ± 12.0[b]	44 ± 18	61 ± 50[b]	48 ± 48[ab]	103 ± 26[b]	11 ± 12[ab]	40 ± 18[c]	52 ± 19[a]	124 ± 31[a]	27 ± 16[c]
3p21 Group (8/8)	5.2 ± 5.9[a]	39 ± 15	48 ± 28[b]	26 ± 26[b]	98 ± 30[b]	6 ± 7[b]	57 ± 17[b]	37 ± 14[b]	94 ± 39[b]	47 ± 16[b]
P value	.0015	.435	.0003	.0138	<.0001	.0061	<.0001	.0041	.0025	<.0001

Individuals in the apoB-defective families were identified previously (Refs. [8,9]). The 3p21 subjects were as follows: family 053 (F family): subjects 541, 547, 549, 559, 571, 575, 577, and 580; family 004: subjects 034, 036, 038, and 039; family 002: subject 013; family 007: subjects 062, 068, and 069. The analyses of variance were done using SAS PROC GLM, and Duncan multiple range tests were done using overall $\alpha = .01$. Superscripts indicate statistical significance. Superscripts that differ from each other by column indicated that means were statistically different.

Table 2
Comparison of VLDL apoB and TG kinetic parameters in 3 groups

Group	VLDL apoB pool size (mg/kg)	VLDL apoB FCR (pools per day)	VLDL apoB PR (mg · kg^{-1} · d^{-1})	VLDL TG Pool size (μmol/kg)	VLDL TG FCR (pools per hour)	VLDL TG PR (μmol · kg^{-1} · h^{-1})
ApoB truncation	0.57 ± 0.36^{a}	11.56 ± 3.87^{b}	5.75 ± 1.83^{b}	10.74 ± 6.90^{b}	1.06 ± 0.74^{b}	9.28 ± 6.04^{b}
3p21	0.51 ± 0.36^{a}	36.48 ± 32.53^{a}	11.42 ± 4.33^{b}	4.45 ± 3.28^{b}	2.69 ± 1.78^{a}	8.23 ± 4.52^{b}
Control	2.76 ± 3.28^{a}	19.79 ± 18.45^{ab}	24.33 ± 12.01^{a}	23.42 ± 12.01^{a}	1.02 ± 0.50^{b}	21.56 ± 9.77^{a}

Duncan multiple comparison was done at $\alpha = .05$. Data recalculated from Refs [18] and [19]. Superscripts within the same column that differ from each other indicated statistically significantly different means.

Different threshold values were assigned to each compartment. The total number of pixels in 8 slices was calculated for each compartment. The number of pixels was converted into volume. Average volume per slice was calculated. From this average, volume average mass of adipose tissue (in kilograms) per slice was derived (assuming that adipose tissue is composed of 84.67% fat, 12.67% water, and 2.66% proteins, and the density of adipose tissue is 0.9196 kg/L [15,16]). Thus, mass of fat per slices equals average volume of adipose tissue in liter × 0.846 × 0.9196.

2.3. Liver fat by MRS

As reported previously, a 1.5-T Siemens Magneton Vision scanner (Siemens) was used with a body radiofrequency (RF) coil as a transmitter and a small flex coil as a receiver. A localized volume MR technique based on a double-spin echo PRESS sequence [17] without water suppression was used. Accurate voxel localization was achieved by using specially designed numerically optimized RF pulses [18]. For accurate quantification of low-intensity fat signal in the presence of the strong signal from water (dynamic range problem), a digital low-pass Savitszky-Golay filter with bandwidth of 30 Hz centered at water resonance frequency was applied to model the strong water time domain signal. Bayesian probability theory was used for further data analysis of digitally separated water and fat signals (Bayesian programs were written by Dr G. Larry Bretthorst). Data were analyzed by modeling the water and fat signals each as an exponentially decaying sinusoid.

Three 2 × 2 × 2 cm voxels were examined in each subject. Two data sets with spin echo times 23 and 53 milliseconds were obtained from each voxel and used to evaluate the spin density for fat and water contributions. The MRS liver fat percent was reported as the spin density of the aliphatic ^{1}H signal divided by the sum of the spin densities of aliphatic plus water ^{1}H signals. The regression of weight-percent liver TG (chemical) on MRS liver fat percent was $y = 0.807x$, $R^2 = 0.986$ [1].

2.4. Statistical analysis

Analyses were performed with SAS (SAS Institute, Cary, NC). Results were presented as means ± SD. Correlation coefficients were performed according to Pearson. The χ^2 test was used to compare sex differences between FHBL and control groups, and the Kruskal-Wallis to compare age differences. The PROC GLM and, once significance was achieved at $P < .01$, the Duncan multiple range tests were used to compare the means of each group with overall α level of .05 or .01 as indicated. Multivariate stepwise regression was used to determine the independent sources of liver fat variation among groups, with MRS liver fat percent or log–liver fat percent as the dependent variable. The values for liver fat percent are presented as measured, without adjustments for covariates, for example, age, BMI, etc.

3. Results

Liver fat contents of the "3p21-linkage" group were significantly lower than in apoB-defective FHBL subjects and resembled those of controls (Table 1). Although both FHBL groups had very low levels of LDL cholesterol and apoB compared with controls, the 3p21 group had higher apoB and LDL cholesterol levels and lower apoA1 and high-density lipoprotein cholesterol levels than the apoB-defective group (Table 1).

VLDL-TG and VLDL-apoB kinetics are presented in Table 2. Mean VLDL-TG FCRs for 3p21 and apoB-defective FHBL subjects were reported as 2.69 versus 1.06 pools per hour, respectively ($P < .05$); control values were 1.02. Respective mean VLDL-apoB FCRs were 36.48 versus 11.56 pools per day ($P < .05$); controls were 19.79, not significantly different from either FHBL groups. Thus, the 3p21 group had higher FCRs for both VLDL-TG and VLDL-apoB. VLDL-apoB production rates were similar in both FHBL groups, but lower than in control (Table 2).

To assess whether the relatively normal liver fat contents in 3p21 were caused by low degrees of adiposity, various

Table 3
Correlations between indices of adiposity, abdominal fat masses, and age in the 3 groups

Variables	SAT	RPAT	IPAT	Age
BMI				
Control	0.664 (<.001)	0.743 (<.001)	0.711 (<.001)	0.253 (.120)
ApoB	0.800 (<.001)	0.690 (<.001)	0.669 (<.001)	0.254 (.147)
3p21	0.745 (<.001)	0.693 (.003)	0.841 (<.001)	0.314 (.199)
W/H ratio				
Control	0.193 (.272)	0.462 (.006)	0.514 (.002)	−0.056 (.737)
ApoB	0.518 (.008)	0.696 (<.001)	0.717 (<.001)	0.268 (.131)
3p21	0.439 (.101)	0.717 (.003)	0.758 (.001)	0.110 (.673)
Age				
Control	0.132 (.454)	0.441 (.009)	0.309 (.007)	–
ApoB	0.479 (.016)	0.674 (<.001)	0.669 (<.001)	–
3p21	0.269 (.312)	0.407 (.117)	0.148 (.584)	–

Table 4
Correlations between liver fat contents and indices of adiposity, as well as abdominal fat masses in the study subjects

Subjects	BMI	W/H ratio	SAT	RPAT	IPAT
Control	0.435	0.236	0.313	0.417	0.569
	39	38	34	34	34
	.056	.154	.071	.014	<.001
ApoB	0.570	0.477	0.423	0.594	0.652
	33	32	25	25	25
	<.001	.006	.035	.002	<0.001
3p21	0.543	0.469	0.514	0.642	0.848
	14	14	14	14	14
	.020	.057	.060	.013	<.001

The numbers in the cells are correlation coefficient, sample size, and P value.

Table 5
Correlations between liver fat content and indices of insulin action in the 3 groups

Subjects	Basal glucose	Basal insulin	AUC glucose	AUC insulin	HOMA
Control	0.272	0.428	0.358	0.567	0.453
	38	37	37	36	37
	.098	.008	.030	<.001	.005
ApoB	0.328	0.518	0.031	0.631	0.533
	30	30	29	29	30
	.076	.003	.872	<.001	.002
3p21	−0.311	0.045	0.240	0.584	0.693
	16	16	14	14	14
	.223	.867	0.408	.028	.006

The numbers in the cells were expressed as correlation coefficients, sample size, and P value.

indices of adiposity were measured. No significant differences were found in the mean values for BMI, waist/hip (W/H) ratio, SAT, RPAT, IPAT, or age between the 3p21 and the other 2 groups (data not shown). Compatible with previous reports [2], significant correlations were present between all measures of adiposity in the 3p21 group (Table 3), but the highest numerical correlations were with IPAT.

As for liver fat, significant correlations were present between it and nearly all indices of obesity (BMI and W/H ratio; Table 4). However, liver fat was most strongly and positively correlated with IPAT. Most importantly, on regression analysis of liver fat on IPAT, the regression line for 3p21 was steeper than the line for controls (Fig. 1, P = .002), although the intercept was similar (P = .137). The slope for the 3p21 group was not significantly different from apoB-defective group (P = .292), but the intercept for the apoB-defective FHBL subjects was significantly higher than for the other 2 groups (P = .014).

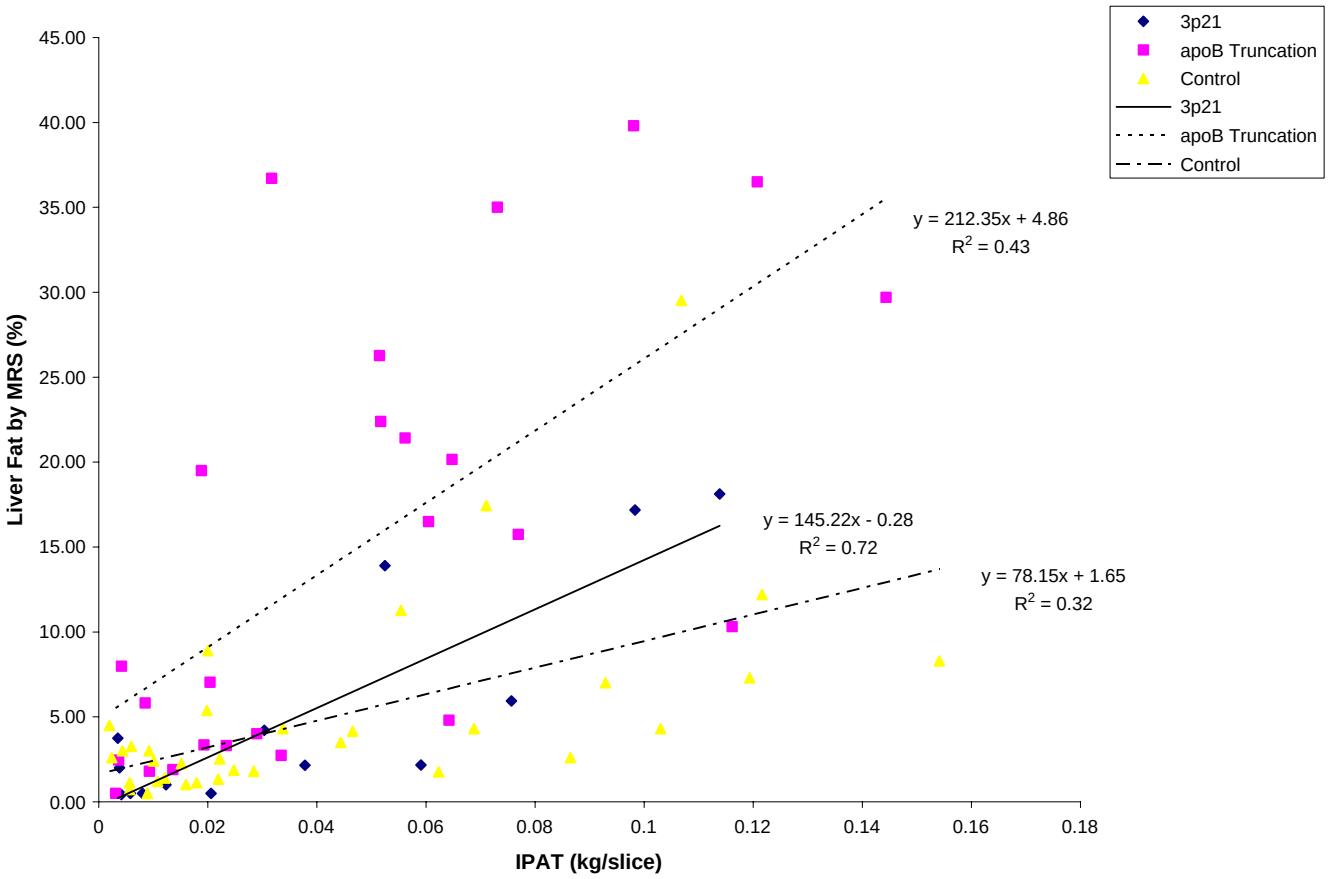

Fig. 1. Simple linear regression between liver fat content (%) and IPAT among the 3 study groups. The t test was used to compare the significant differences among the 3 slopes of the regression equations. There were significant differences between slopes of control and apoB-defective equation, as well as control and 3p21 equation (P < .001), but there was no difference between apoB-defective and 3p21 group (P = .292). Intercepts differed between the apoB-defective and the other 2 groups, but not between the 3p21 and controls (P = .134).

Table 6
Multiple variant regression analysis using liver fat as dependent variable

Patient group	Model R^2	Independent variables	Partial R^2	P value
ApoB Truncation (N = 27)	0.92	IPAT	0.57	<.001
		LDL	0.25	<.001
		ALT/AST	0.05	.022
		HOMA	0.05	.006
3p21 (N = 11)	0.57	IPAT	0.57	.007
Control (N = 31)	0.42	AUC insulin	0.33	<.001
		Age	0.09	.043

ALT indicates alanine aminotransferase; AST, aspartate aminotransferase.

Next, we examined the role of insulin sensitivity on liver fat. There were no significant differences of indices of insulin action, that is, basal glucose, basal insulin, AUC glucose, AUC insulin, and HOMA, among the 3 groups (data not shown), suggesting that differences in insulin action per se did not account for differences in liver fat content. Liver fat contents were significantly correlated with several indices of insulin action in all 3 groups (Table 5), most notably with the AUC insulin and HOMA.

On stepwise regression analysis, the strongest correlate for liver fat in apoB-defective subjects was IPAT, followed by LDL cholesterol (Table 6). In controls, the numerically highest correlates were measures of insulin action, whereas in the 3p21 group, the highest correlates were also IPAT and LDL cholesterol.

4. Discussion

Our major finding is the absence of hepatic steatosis in the 3p21 participants, in contrast with the apoB-defective group (Table 1). Other phenotypic differences between the 2 FHBL groups have been noted in lipoprotein levels (Table 1) and with respect to VLDL-TG and VLDL-apoB kinetic parameters (Table 2) [10,11]. The FCRs of both VLDL components were higher in the 3p21 group than in the apoB-defective or control subjects. Mean VLDL-apoB production rates were similar in 3p21 and in apoB-defective FHBL subjects, both were lower than controls. The kinetic data are compatible with a higher rate of flux of VLDL particles into and through plasma in the 3p21 group compared with apoB-defective group.

VLDL assembly and secretion are complex processes [19]. The synthesis of the major classes of lipids and of apoB is followed by the cotranslational assembly of lipids and apoB into primary particles in the rough endoplasmic reticulum (ER). The assembly requires microsomal triacylglycerol transfer protein [20]. Further lipid loading occurs in the smooth ER. Transport in coat protein complex II vesicles moves the VLDL from ER to the Golgi where further lipid loading occurs [21-23]. Then, VLDL proceeds through a secretory pathway that may contain LDL receptors [24,25]. The receptors may remove smaller (perhaps incompletely lipidated) particles for intracellular degradation and permit larger ones to be secreted into plasma. In plasma, VLDL particles are subject to lipolysis catalyzed by either lipoprotein lipase or hepatic TG lipase, located at the luminal surfaces of vascular endothelial cells, which converts them to intermediate-density lipoprotein and LDL particles [26]. Particles are removed at every step of the "lipolytic cascade" via endocytosis, mediated by LDL receptors or apoE receptors. Whether the VLDL of 3p21 subjects is abnormally rapidly cleared directly or after convertion via lipolysis to intermediate-density lipoprotein and LDL remains to be determined. At any rate, the modestly reduced production rates for VLDL-apoB and VLDL-TG and the rapid clearance/conversion of VLDL in plasma suggest that some alteration may be occurring in intracellular VLDL production that may render the particles susceptible to postsecretory "special handling" resulting in rapid removal. Alternatively, the increased lipolysis of VLDL-TG catalyzed by hepatic TG lipase may be occurring right after secretion, for example, in the space of Disse, followed by reuptake of the resultant VLDL "remnants" by hepatocytes.

One of our aims was to assess whether and to what extent indices of adiposity predicted liver fat contents in the 3p21 group. Liver fat contents rose with increasing abdominal adiposity in all 3 genetic groups. However, in both FHBL groups, for any given rise in adiposity, liver fat rises disproportionately compared with controls (Fig. 1), and the rise is significantly greater for the apoB-defective than for the 3p21 subjects.

It is not clear how the sizes of the fat depots may affect VLDL production, whether by provision of free fatty acid substrates or hormonal effects [27], but our data suggest that the susceptibilities of the livers to abdominal tissue effects are ranked apoB-defective > 3p21 > controls. Thus, we have observed still another phenotypic difference between the forms of FHBL under study. The increased susceptibility of apoB-defective FHBL subjects to the effects of adiposity is explainable by the *APOB* defects that limit the TG transporting capacity of the VLDL export system [1,2,28]. No genetic explanation is yet available for the 3p21 group because the gene(s) has not yet been identified.

Because indices of adiposity, insulin action, and liver fat are correlated in obese and diabetic subjects, we sought correlations between insulin action and liver fat in our subjects. There were positive correlations between indices of insulin action and liver fat contents in all groups. This probably reflects (a) the decreasing effectiveness of insulin in suppressing hormone-sensitive lipase catalyzed lipolysis in adipose tissue by increasing degrees of insulin resistance and (b) the increasing effects of hyperinsulinemia on hepatic TG synthesis [29]. However, the pattern of correlations differed by group. Fasting glucose and insulin levels did not correlate with liver fat in the 3p21-linked group, whereas it did in the other 2 groups. The AUC glucose did not correlate with liver fat in apoB-group, whereas it did in the others (Table 5). The absence of uniform patterns of correlations in the 3 groups was reflected on multivariate analysis. The independent variables differed for the 2 FHBL groups and

for controls. Thus, the 2 genetic forms differ from each other in a number of phenotypic features.

The "3p21" region defined by crucial crossovers in our 3p21 families includes approximately 120 genes. Many of these are genes related to immune responses, such as a cluster of chemokine receptors [30]. This region also partially overlaps with the chromosome 3 common eliminated region 1 (C3CER1) on 3p21.3 [31] frequently observed in cancers. There are several candidate genes associated with lipid metabolism, such as the sterol 12α-hydroxylase gene (*CYP8B1*), *Homo sapiens* SEC22 vesicle trafficking protein-like (*SEC22L*), vasoactive intestinal peptide receptor 1 (*VIPR1*), zinc-finger protein genes, and several protein kinase genes. The sterol 12α-hydroxylase is a key enzyme involved in the cholic acid biosynthetic pathway. Disruption of this gene interrupts cholesterol metabolism in both human and mice [32,33]. The *Saccharomyces cerevisiae* Sec22 plays a role in ER to Golgi transport [34]. Zinc-finger genes encode metal-binding proteins that can act as transcriptional regulators of other genes, whereas protein kinases are involved in gene regulations [35]. Which, if any, of these genes is involved in the FHBL in our 3p21 patients remained to be determined.

Acknowledgments

The authors appreciate the cooperation of our study subjects and the interactions of Jackie Dudley, RN, with them. The funding was provided by NIH HL RO1-59515, NIH HL R37-42460, NIH RR-00036 (General Clinical Research Center), NIH DK56341 (Clinical Nutrition Research Unit), and NIH RR-00954 (Biomedical Mass Spectrometry Resource).

References

[1] Schonfeld G, Patterson BW, Yablonskiy DA, et al. Fatty liver in familial hypobetalipoproteinemia: triglyceride assembly into VLDL particles is affected by the extent of hepatic steatosis. J Lipid Res 2003;44:470-8.

[2] Tanoli T, Yue P, Yablonskiy D, et al. Fatty liver in familial hypobetalipoproteinemia: Roles of the APOB defects, intra-abdominal adipose tissue, and insulin sensitivity. J Lipid Res 2004;45:941-7.

[3] Tarugi P, Lonardo A. Heterozygous familial hypobetalipoproteinemia associated with fatty liver. Am J Gastroenterol 1997;92:1400-2.

[4] Tarugi P, Lonardo A, Ballarini G, et al. A study of fatty liver disease and plasma lipoproteins in a kindred with familial hypobetalipoproteinemia due to a novel truncated form of apolipoprotein B (APO B-54.5). J Hepatol 2000;33:361-70.

[5] Schonfeld G. Familial hypobetalipoproteinemia: A review. J Lipid Res 2003;44:878-83.

[6] Young SG. Recent progress in understanding apolipoprotein B. Circulation 1990;82:1574-94.

[7] Burnett JR, Shan J, Miskie BA, et al. A novel nontruncating APOB gene mutation. R463W, causes familial hypobetalipoproteinemia. J Biol Chem 2003;278:13442-52.

[8] Yuan B, Neuman R, Duan SH, et al. Linkage of a gene for familial hypobetalipoproteinemia to chromosome 3p21.1-22. Am J Hum Genet 2000;66:1699-704.

[9] Neuman RJ, Yuan B, Gerhard DS, et al. Replication of linkage of familial hypobetalipoproteinemia to chromosome 3p in six kindreds. J Lipid Res 2002;43:407-15.

[10] Elias N, Patterson BW, Schonfeld G. Decreased production rates of VLDL triglycerides and apoB-100 in subjects heterozygous for familial hypobetalipoproteinemia. Arterioscler Thromb Vasc Biol 1999;19:2714-21.

[11] Elias N, Patterson BW, Schonfeld G. In vivo metabolism of apoB, apoA-I, and VLDL triglycerides in a form of hypobetalipoproteinemia not linked to the apoB gene. Arterioscler Thromb Vasc Biol 2000;20:1309-15.

[12] Hoyumpa Jr AM, Greene HL, Dunn GD, et al. Fatty liver: Biochemical and clinical considerations. Am J Dig Dis 1975;20:1142-70.

[13] National Institutes of Health. Manual of laboratory operations lipid research clinic program in lipid and lipoprotein analysis. Bethesda, Md: NIH; 1982.

[14] Contois JH, McNamara JR, Lammi-Keefe CJ, et al. Reference intervals for plasma apolipoprotein B determined with a standardized commercial immunoturbidimetric assay: results from the Framingham Offspring Study. Clin Chem 1996;42:515-23.

[15] Abate N, Garg A, Coleman R, et al. Prediction of total subcutaneous abdominal, intraperitoneal, and retroperitoneal adipose tissue masses in men by a single axial magnetic resonance imaging slice. Am J Clin Nutr 1997;65:403-8.

[16] Abate N, Burns D, Peshock RM, et al. Estimation of adipose tissue mass by magnetic resonance imaging: validation against dissection in human cadavers. J Lipid Res 1994;35:1490-6.

[17] Bottomley PA. Spatial localization in NMR spectroscopy in vivo. Ann N Y Acad Sci 1987;508:333-48.

[18] Raddi A, Klose U. A generalized estimate of the SLR B polynomial ripples for RF pulse generation. J Magn Reson 1998;132:260-5.

[19] Shelness GS, Sellers JA. Very-low–density lipoprotein assembly and secretion. Curr Opin Lipidol 2001;12:151-7.

[20] Read J, Anderson TA, Ritchie PJ, et al. A mechanism of membrane neutral lipid acquisition by the microsomal triglyceride transfer protein. J Biol Chem 2000;275:30372-7.

[21] Jones B, Jones EL, Bonney SA, et al. Mutations in a Sar1 GTPase of COPII vesicles are associated with lipid absorption disorders. Nat Genet 2003;34:29-31.

[22] Shelness GS, Ingram MF, Huang XF, et al. Apolipoprotein B in the rough endoplasmic reticulum: translation, translocation and the initiation of lipoprotein assembly. J Nutr 1999;129:456S-62S.

[23] Siddiqi SA, Gorelick FS, Mahan JT, et al. COPII proteins are required for Golgi fusion but not for endoplasmic reticulum budding of the pre-chylomicron transport vesicle. J Cell Sci 2003;116:415-27.

[24] Gillian-Daniel DL, Bates PW, Tebon A, et al. Endoplasmic reticulum localization of the low density lipoprotein receptor mediates presecretory degradation of apolipoprotein B. Proc Natl Acad Sci U S A 2002;99:4337-42.

[25] Larsson SL, Skogsberg J, Bjokegren J. The low density lipoprotein receptor prevents secretion of dense apoB100-containing lipoproteins from the liver. J Biol Chem 2004;279:831-6.

[26] Fielding PE, Fielding CJ. Dynamics of lipoprotein transport in the human circulatory system. In: Vance DE, Vance JE, editors. Biochemistry of Lipids, Lipoproteins and Membranes. Amsterdam: Elsevier Science; 1996. p. 495-517.

[27] Kahn BB, Flier JS. Obesity and insulin resistance. J Clin Invest 2000;106:473-81.

[28] Lin X, Schonfeld G, Yue P, et al. Hepatic fatty acid synthesis is suppressed in mice with fatty livers due to targeted apolipoprotein B38.9 mutation. Arterioscler Thromb Vasc Biol 2002;22:476-82.

[29] Mason TM, Chan B, El-Bahrani B, et al. The effect of chronic insulin delivery via the intraperitoneal versus the subcutaneous route on hepatic triglyceride secretion rate in streptozotocin diabetic rats. Atherosclerosis 2002;161:345-52.

[30] Papadakis KA, Landers C, Prehn J, et al. CC chemokine receptor 9 expression defines a subset of peripheral blood lymphocytes with mucosal T cell phenotype and Th1 or T-regulatory 1 cytokine profile. J Immunol 2003;171:159-65.

[31] Kiss H, Yang Y, Kiss C, et al. The transcriptional map of the common eliminated region 1 (C3CER1) in 3p21.3. Eur J Hum Genet 2002;10: 52-61.

[32] Pullinger CR, Eng C, Salen G, et al. Human cholesterol 7alpha-hydroxylase (CYP7A1) deficiency has a hypercholesterolemic phenotype. J Clin Invest 2002;110:109-17.

[33] Li-Hawkins J, Gafvels M, Olin M, et al. Cholic acid mediates negative feedback regulation of bile acid synthesis in mice. J Clin Invest 2002;110:1191-200.

[34] Parlati F, McNew JA, Fukuda R, et al. Topological restriction of SNARE-dependent membrane fusion. Nature 2000;407:194-8.

[35] Manning G, Whyte DB, Martinez R, et al. The protein kinase complement of the human genome. Science 2002;298:1912-34.